Energy & Environmental Science

An ultrafast process for fabrication of Li metal–inorganic solid electrolyte interface

Journal:	*Energy & Environmental Science*
Manuscript ID	EE-ART-03-2021-000759.R2
Article Type:	Paper
Date Submitted by the Author:	04-Jun-2021
Complete List of Authors:	Kitaura, Hirokazu; National Institute of Advanced Industrial Science and Technology Tsukuba Central 2, Research Institute for Energy Conservation Hosono, Eiji; National Institute of Advanced Industrial Science and Technology Tsukuba West, Research Institute for Energy Conservation; National Institute of Advanced Industrial Science and Technology Tsukuba West, Global Zero Emission Research Center Zhou, HaoShen; National Institute of Advanced Industrial Science and Technology Tsukuba Central 2, Research Institute for Energy Conservation

ARTICLE

An ultrafast process for fabrication of Li metal–inorganic solid electrolyte interface

Received 00th January 20xx,
Accepted 00th January 20xx

DOI: 10.1039/x0xx00000x

Hirokazu Kitaura,*[a] Eiji Hosono [a,b] and Haoshen Zhou [a]

Lithium anode is expected to be applied to next-generation batteries using inorganic solid electrolytes (ISEs). When joining Li with ISEs, interfacial reactions often cause performance degradation and has been avoided. In this report, we demonstrate a new strategy of ultrafast formation of good interface between Li and ISEs, using a reactive process (ultrasonic-assisted fusion welding method). We found that ultrasonic irradiation helps the suitable interface formation reactions between molten Li and ISE, and the joining process finish in just a few seconds. An obtained interface showed a low resistance and enabled to use under the high current density of 0.5 mA cm^{-2}. The development of prototype cells for next-generation batteries was promoted by this ultrafast process.

Introduction

In recent years, research on inorganic solid electrolytes (ISEs) has attracted attention, especially towards the commercialization of all-solid-state batteries for electric vehicles[1]. Li metal is regarded as the ultimate anode material due to their excellent characteristics of a large theoretical capacity of 3860 mAh g^{-1} and a negative potential of −3.04 V (vs. standard hydrogen electrode)[2]. The combination of ISE and Li is expected to realize next-generation batteries that combine safety and high energy density. However, conventional ISEs have a problem that they metamorphose into low ion-conductive phases when contacted with highly reactive Li metal[3,4]. The discovery of a solid electrolyte system of $Li_7La_3Zr_2O_{12}$ (LLZ) stable to Li metal motivated further work on a combination of ISE and Li metal[5-7]. In the midst of this, it has been found that LLZ is a challenging material that is difficult to join to Li metal[8]. According to the reports, this is mainly due to the impurities of Li_2CO_3 and LiOH that naturally forms on the surface by a reaction of LLZ and moisture[9,10]. The impurity layer has poor wettability with molten Li and interferes with the interface formation of LLZ with Li metal. Therefore, high resistance due to poor contact between LLZ and Li will be observed.

To solve this problem, the surface of LLZ has been controlled in various ways, and especially following two kinds of approaches have succeeded in significantly reducing the resistance. One is the approach to remove the impurity phase before joining with Li. Sharafi *et al*. carefully removed the impurity phase by wet polishing and heat treatment and demonstrated that it improves the molten Li wettability and interfacial resistance[9]. The other is the approach to introduce the coating layer on the LLZ surface. Han *et al*. coated the LLZ surface with Al_2O_3 thin film by atomic layer deposition (ALD)[11]. The coating layer not only improves the molten Li wettability but can also provide additional function, such as mixed conduction of ion and electron[12]. On the other hand, these approaches can require additional long and cumbersome processes compared to the case of simple fusion welding. Therefore, it takes a huge amount of time to make trial and error in research that requires various battery tests. We thought that in order to accelerate research and development in this field, a simple method that can join in a short time is necessary.

To achieve the above goal, we adopted a new strategy of aggressively using technology for promoting the joining between Li metal and ISE. Specifically, ultrasonication was used. It was reported that the chemical bonding between ceramics and metals is closely related to the joining[13], and it was also reported that ultrasonication during heat treatment has the effect of promoting the formation of such chemical bonding[14]. On the other hand, since the interfacial reactions between solid electrolytes and electrode materials often gives undesirable results such as structural degradation and high interfacial resistance, it has been considered as a common recognition in this field that the interfacial reactions should be avoided[3,4,15]. Therefore, since there was a possibility that the aggressively promoting joining by ultrasonication and heat treatment cause deterioration of the interface, such strategy has been avoided.

In this study, we report that this new strategy is sufficiently useful for interfacial formation for batteries. Molten Li was joined with LLZ by the ultrasonication. On this work, we refer to the technology as ultrasonic-assisted fusion welding (UFW) method. By the UFW method, Li and LLZ can be joined in a few seconds, and it was found that an interface with characteristics

[a] *Research Institute for Energy Conservation, National Institute of Advanced Industrial Science and Technology (AIST), Umezono 1-1-1, Tsukuba, Ibaraki 305-8568, Japan.*
[b] *Global Zero Emission Research Center, National Institute of Advanced Industrial Science and Technology (AIST), Umezono 1-1-1, Tsukuba, Ibaraki 305-8568, Japan.*

† Electronic Supplementary Information (ESI) available: [Fig. S1-S6, Movie S1-S2]. See DOI: 10.1039/x0xx00000x

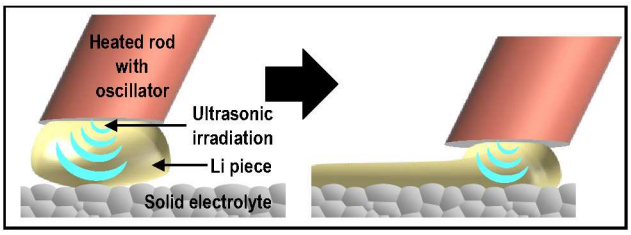

Fig. 1. Scheme of the ultrasonic-assisted fusion welding method.

comparable to the conventional interface formation method can be formed. Also, using this easily fabricated Li-LLZ, we developed two kinds of the next-generation battery prototypes.

Results and discussion

Joining characteristics of UFW method

An outline of UFW method is shown in Fig. 1. A molten piece of Li on a heated stainless-steel rod is appressed to the ISE surface, and the Li is then irradiated with ultrasonic waves using an ultrasonic transducer attached to the heated rod for a few seconds. We investigated the appropriate conditions as described in the experimental section. It is important to find the appropriate conditions about temperature, output, and irradiation time. For example, when the irradiation time is too long, crack may appear in the substrate. We applied this method to a glass substrate as a proof of principle. When the ultrasonic wave is not irradiated (Supplementary Movie 1), it is confirmed that the surface of the glass substrate repels Li metal. On the other hand, using the ultrasonic irradiation, the Li metal is uniformly bonded to the surface of the substrate in a few seconds as shown in Supplementary Movie 2. Since the Li metal is strongly joined, it was difficult to peel off it from the glass substrate. During ultrasonic irradiation, molten Li can be applied extensively to the surface of the substrate by moving the rod. In this way, Li metal can be applied in a user-defined pattern (Fig. 2a). The thickness of Li depends on the loaded (or provided) molten Li. When the thickness should be controlled more strictly, it may be better to use a Li sheet of the desired thickness and a heating stage with an oscillator instead of a moving rod.

The reaction between Li and SiO_2 was confirmed by X-ray photoelectron spectroscopy (XPS). A reaction region with a concentration gradient of Li and Si in the XPS depth profile (Fig. 2b) was observed over the sputtering timeframe of 0 to 30 min. Two peaks were observed in the Si 2*p* spectra (Fig. S1). The peaks around 100 eV and 104 eV can be assigned to Li-O-Si bond and Si-O-Si bond, respectively[16]. The peak shift of Li-O-Si corresponds to the composition change from Li-rich lithium silicate (Li_4SiO_4) to Li-poor lithium silicate (Li_2SiO_3). These results demonstrate that the joining reactions were promoted by ultrasonic irradiation.

We carried out the Li formation on the LLZ disc by the UFW method. As a control sample, Li was joined with LLZ disc by the conventional fusion welding (FW) method without ultrasonication. First, the surface of LLZ was roughly polished with a polishing paper in a glove box to remove an excess impurity layer, and then Li was joined with LLZ in each method.

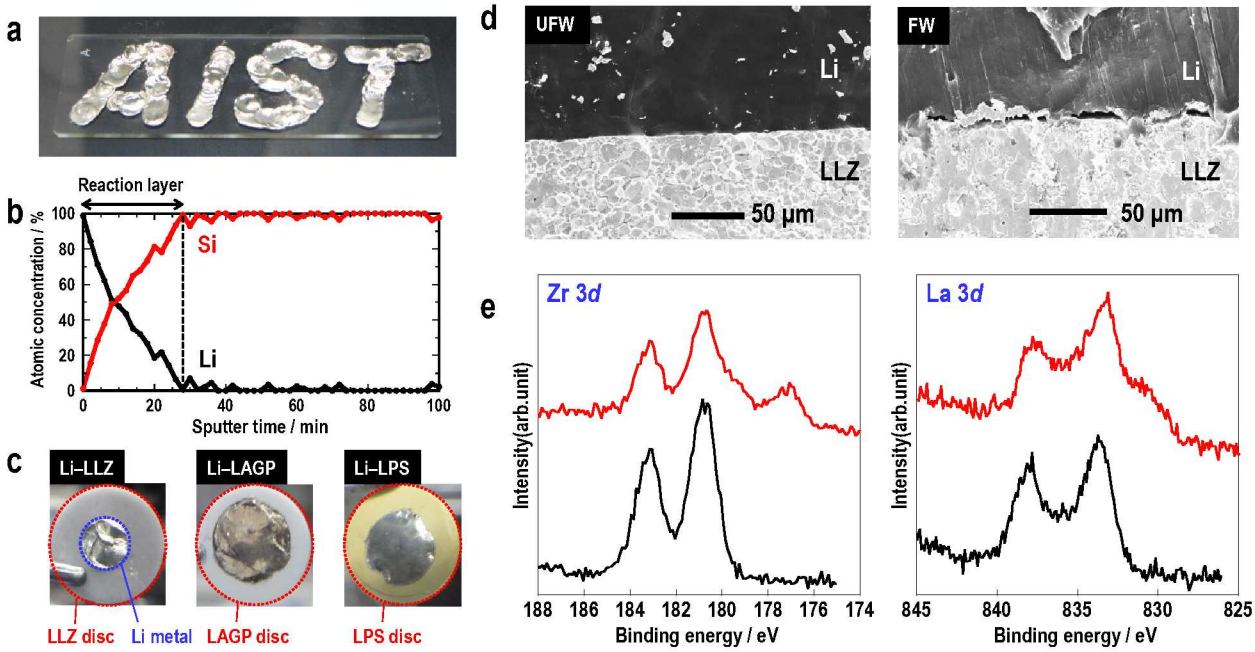

Fig. 2. Profile of the UFW method. (a) Photograph of Li formed on a glass slide. (b) Depth profile of atomic concentration for Li–SiO_2. (c) Photographs of Li–ISEs using LLZ, LAGP and LPS discs. (d) Fracture cross-sectional SEM images of Li–LLZ interfaces constructed by the UFW and FW methods. (e) Zr 3*d* and La 3*d* XPS spectra of the surface of polished LLZ (black line) and Li–LLZ interface constructed by the UFW method (red line).

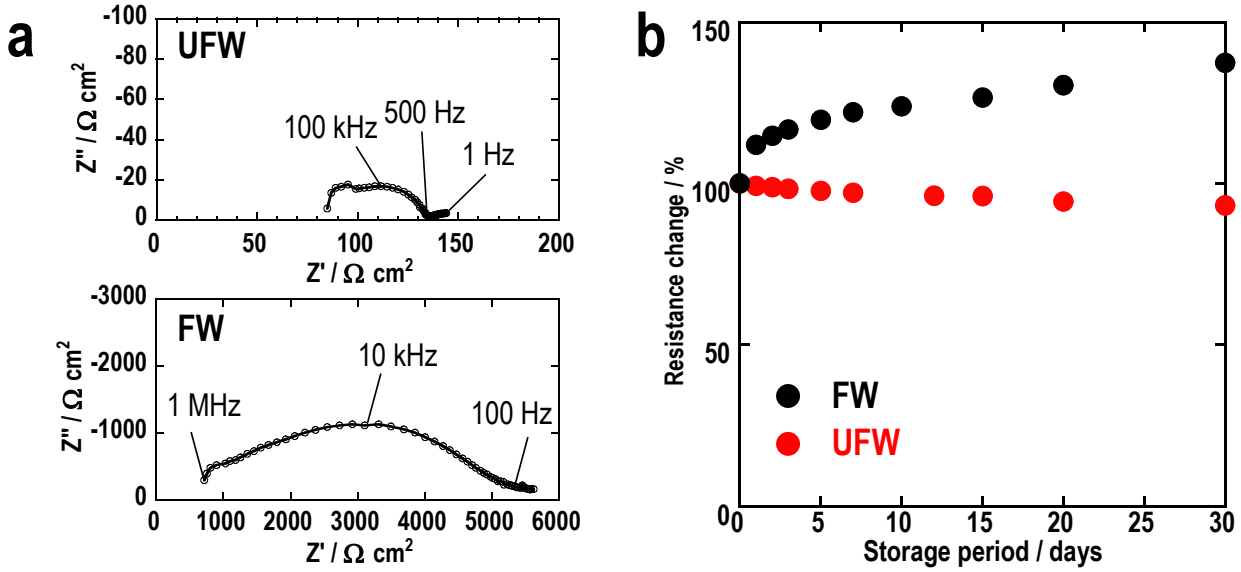

Fig. 3. Characterization of the resistance in the Li symmetric cells. (a) Impedance spectra of the UFW- and FW-fabricated cells at 30 °C. (b) Resistance change of the UFW- and FW-fabricated cells stored at 30 °C.

In the XPS measurement of the surface after polishing, it was confirmed that the impurity layer is still remaining (Fig. S2). As described above, such surface has poor wettability with molten Li, and it is difficult to join them[9]. Nevertheless, in the UFW method, it was possible to easily join Li and LLZ (Fig. 2c), and they were strongly joined similar to the case of Li and SiO_2. The state of the interface formation can be clearly observed in the cross-sectional scanning electron microscopy (SEM) images (Fig. 2d). In the FW method, voids were observed at the interface, and Li is easily exfoliated from the surface of the LLZ disc by tweezers. On the other hand, in the UFW method, it was observed that the interface between LLZ and Li was in close contact. The XPS measurements of the Li–LLZ interface constructed by the UFW method were performed and compared with the surface of the polished LLZ disc (Fig 2e and Fig. S3). In the Zr 3*d* and La 3*d* spectra of the Li–LLZ interface, additional peaks in the low energy region were observed, suggesting the formation of reaction products. It is considered that the formation of reaction layer leads to the formation of a close interface between Li and LLZ.

We additionally demonstrate the results of the UFW method applied to the Li_2CO_3 and LiOH discs. (Fig. S4). It was reported that the contact angles of molten Li on Li_2CO_3 and LiOH are 142 ° and 125.3 ° and their molten Li wettability are poor[9]. However, we confirmed that the UFW method enables the joining of molten Li with Li_2CO_3 and LiOH. This result proves that Li can be joined with the LLZ disc even if the impurity layer is not completely removed by ultrasonication. Furthermore, it was possible to form Li on a phosphate ISE of $Li_{1.5}Al_{0.5}Ge_{1.5}(PO_4)_3$ (LAGP) and a sulfide ISE of Li_3PS_4 (LPS) (Fig. 2c). This suggests that the UFW method has potential for application to various ISEs.

Electrical and electrochemical characterization of UFW-fabricated Li-LLZ

The quality of the contact is directly reflected to the electrical and electrochemical performance. On the other hand, the interfacial reactions between Li electrode and ISE sometimes involve a high interfacial resistance along with the growth of an interfacial reaction layer[4,17]. Therefore, the interfacial reactions have been considered to be undesirable for the formation of electrochemically favorable interface. Here we demonstrate that this method has no problem to apply to the Li–LLZ formation. Impedance measurements were conducted in the Li|LLZ|Li symmetrical cells prepared by the UFW and FW methods (Fig. 3a). One obvious semicircle was observed in each plot. A total resistance of 135 Ω cm^2 was measured for the UFW-fabricated cell at 30 °C, much lower than that of approximately 5200 Ω cm^2 for the FW-fabricated cell. To clarify the interfacial resistance (R_{int}) between Li and LLZ in the UFW-fabricated cell, detailed impedance measurement was further conducted by using a high frequency measurement system at room temperature. One additional semicircle was observed in the high frequency region. The fitting of the impedance plot can be performed by an equivalent circuit model shown in Fig. S5 and it was found that the semicircles in the high and low frequency region were ascribed to LLZ itself and Li-LLZ interface, respectively. Therefore, at 30 °C, R_{int} was calculated to 22 Ω cm^2, which is comparable to that of the successful example[11]. In addition, the interfacial resistance of the UFW-fabricated cell did not increase during storage for 1 month at 30 °C (Fig. 3b). These results suggest that even if the interfacial reaction layer is formed in this method, it has limited thickness and does not grow on long-term storage. This is an important finding that the joining between Li and LLZ using a reactive process is effective. On the other hand, the resistance of the FW-fabricated cell

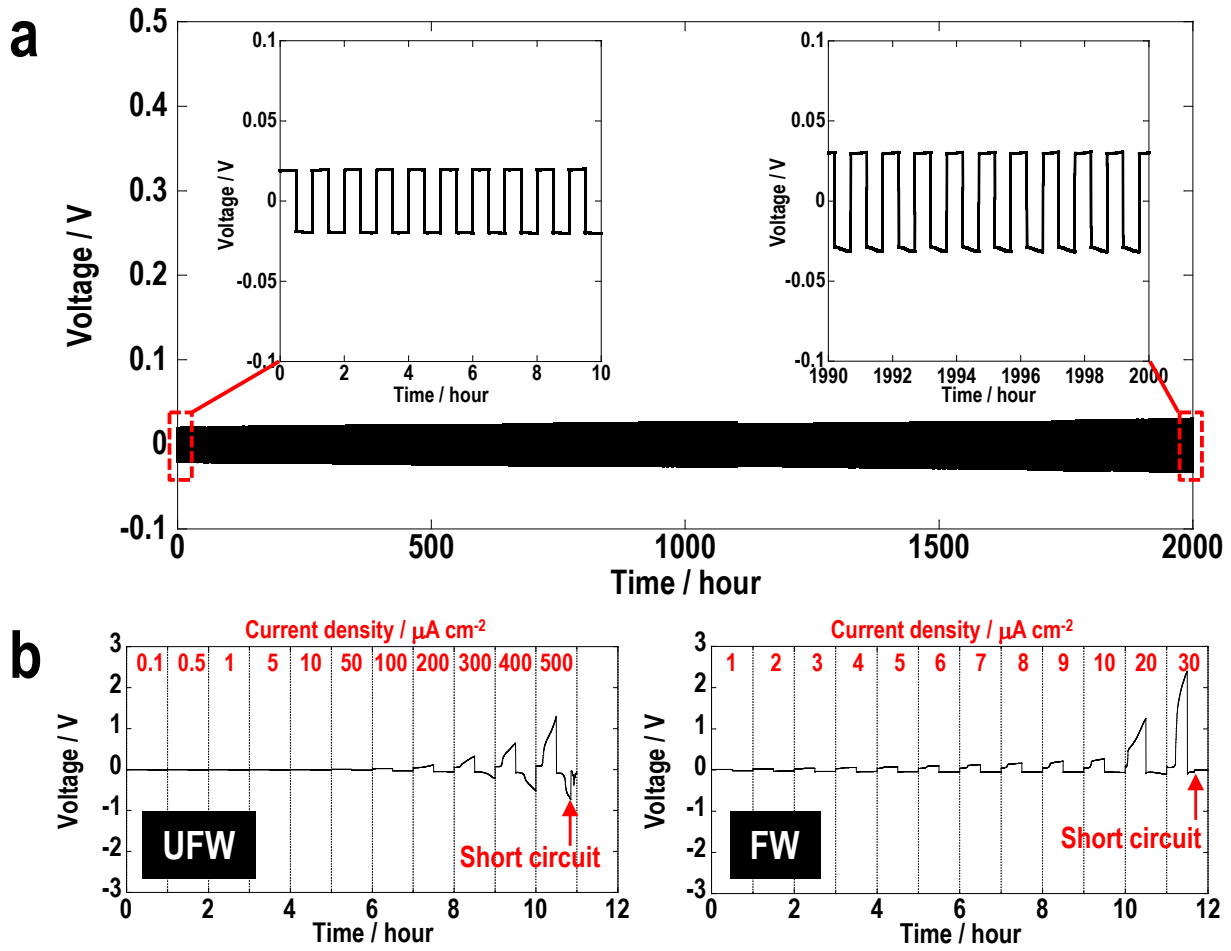

Fig. 4. Characterization of Li deposition and dissolution. (a) Galvanostatic cycling of a UFW-fabricated cell. The insets are enlarged figures of first and last ten hours. (b) Galvanostatic step measurements of the UFW- and FW-fabricated cells. All electrochemical measurements were conducted in Li|LLZ|Li symmetrical cells at 30 °C.

increased during storage. Since LLZ is a very sensitive material against H_2O and CO_2, this may be due to the degradation of LLZ spreading from the surface, which is not completely covered by Li.

The cycle stability of a UFW-fabricated cell was investigated by Li plating and stripping tests (Fig. 4a). Li plating and stripping were each conducted at a current density of 0.1 mA cm^{-2} for 30 min per cycle and the voltage profile was monitored. The UFW-fabricated cell worked over 2000 cycles without short-circuit. Comparing the first ten hours and the last ten hours (Fig. 4a, inset), although a slight increase in overvoltage was observed, the voltage profile was stable without voltage disturbance until the end. The critical current density (CCD) for Li plating and stripping was also investigated (Fig. 4b). The CCD is defined as the lowest current density at which short-circuit occurs due to Li metal penetration[9]. The current density was increased in a stepwise manner described in the upside of Fig. 4b and the voltage profile was monitored. Since the state of interface significantly affects the CCD, the UFW-fabricated cell showed the CCD of 0.5 mA cm^{-2}, which is much higher than the CCD of 0.03 mA cm^{-2} in FW-fabricated cell.

Application of UFW-fabricated Li-LLZ to next-generation batteries.

We applied UFW-fabricated Li–LLZ to two types of usage for next-generation batteries; protected Li electrode and all-solid-state Li-O_2 battery. Protected Li electrode means that ISE is used as a layer for protecting Li electrodes from undesirable reactions with harmful components such as water, reactive gasses and liquid electrolyte components[18-20]. In both types of cells, NASICON-type ISEs have been used to create Li–ISE materials[18-24]. However, since NASICON-type ISEs have significant performance degradation with time when directly contacted with Li metal[4], an interlayer such as polymer electrolytes and nitrogen-doped lithium phosphate (LiPON) thin film ISE, which have low ionic conductivity, is required. Removal of the interlayer by using Li–LLZ is expected to achieve lower resistance and simplification of the cell.

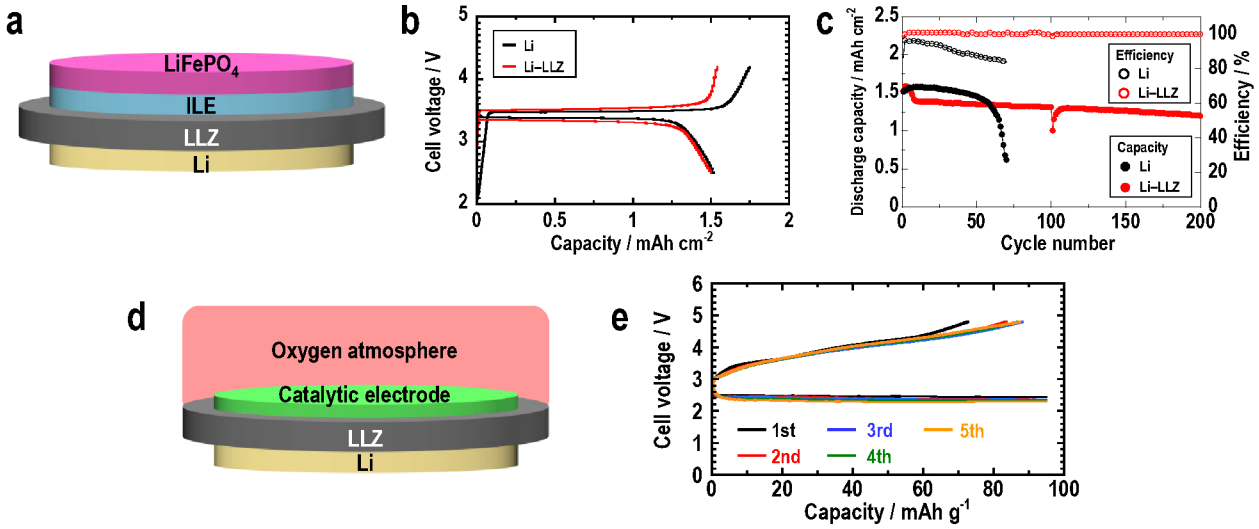

Fig. 5. Electrochemical performances of an ILE cell and an all-solid-state Li–O_2 cell. (a) Schematic diagram of a Li–LLZ|1 M LiTFSI in TEGDME|$LiFePO_4$ ILE cell. (b) First charge–discharge curves of the ILE cells using bare Li electrode (black lines) and protected Li (Li–LLZ) electrode (red lines). (c) Cyclic performance of the ILE cells using bare Li electrode (black circles) and protected Li (Li–LLZ) electrode (red circles). (d) Schematic diagram of an all-solid-state Li|LLZ|catalytic electrode–O_2 cell. (e) Charge–discharge profile of the all-solid-state Li–O_2 cell.

Fig. 5a shows the schematic diagram of a cell using Li–LLZ as a protected Li electrode. We focused on an ionic liquid electrolyte (ILE) of 1 M lithium bis(trifluoromethanesulfonyl)imide (LiTFSI) in tetraethylene glycol dimethyl ether (TEGDME). In the previous report, a cell using the ILE showed capacity degradation during cycling[25]. It is considered that the degradation is mainly caused by the dendritic growth and side reactions of Li metal[25,26]. Therefore, we applied the Li–LLZ to the ILE cell and investigated the effect of Li–LLZ as protected Li electrode. A $LiFePO_4$ cathode was used and a control cell using bare Li is the same constitution as the cell in Ref. 25. Fig. 5b and 5c shows the first charge–discharge curve and cycle performance, respectively, of these two cells. The bare Li-based cell showed low charge–discharge efficiency and capacity degradation over 70 cycles. This observed degradation is consistent with previous research[25]. In contrast, the Li–LLZ-based cell can be charged and discharge without large capacity degradation during 200 cycles. This result demonstrates that Li–LLZ functions as a protected Li anode to suppress undesirable reactions.

A schematic diagram of a cell we constructed with the Li–LLZ and a catalytic electrode is shown in Fig. 5d. Li–O_2 battery has recently received much attention as a next-generation battery due to its high theoretical energy density[27,28]. However, the higher energy stored in a battery, the greater the danger. Therefore, careful safety arrangements are required, and thus, all-solid-state Li–O_2 batteries without flammable organic liquid electrolytes have been studied[21-24]. Since the preparation of Li–LLZ became easy by using the UFW method, the development of a catalytic electrode was promoted. The cell was repeatedly discharged and charged under a current density of 10 mA g^{-1} at 60 °C. The cell worked and showed the typical voltage profile of Li–O_2 cell during cycling (Fig. 5e). To our knowledge, this is the first data of the Li–O_2 cell using LLZ without polymer and liquid components.

Conclusions

Li was joined to LLZ using the UFW method. It was found that a close contact interface is formed in a short time simply by irradiating the molten lithium with ultrasonic waves. In addition, ultrasonication did not cause serious deterioration of the interface, and the total resistance was 135 Ω cm^2, which was dramatically lower than the 5200 Ω cm^2 in the case without ultrasonication. As a result, the symmetric cells produced by this method showed a high CCD of 0.5 mA cm^{-2}. Also, the cell achieved more than 2000 cycles of stable cycling at 0.1 mA cm^{-2}. Moreover, UFW-fabricated Li-LLZs played an important role in the development of prototype cells of protected Li cell and all-solid-state Li-O_2 cell. This work demonstrates the potency of this new strategy of aggressive joining of Li and ISE, and can be expected to be an important technology for accelerating the development of next-generation batteries.

Experimental

Materials

LLZ disc (Toshima Manufacturing Co., Ltd., 15 mm φ, 1 mm thickness), glass slide, SiO_2 glass substrate was obtained. The surface of LLZ disc was polished by the polishing paper #400 in the glove box before joining. LPS glass powder was provided from Inorganic Chemistry group of Osaka Prefecture University.

The LPS powder was pressed at 330 MPa to obtain a disc. LAGP was synthesized by the conventional solid phase method[21].

Joining process

UFW method was conducted using a device (Kuroda Techno Co., Ltd., Sunbonder USM-560) as follows: A molten piece of Li on a heated stainless steel rod is appressed to the ISE surface (or other substrates), and the Li is then irradiated with ultrasonic waves using an ultrasonic transducer attached to the heated rod for a few seconds. Firstly, the suitable condition of temperature and ultrasonic oscillations output was investigated. As shown in Fig. S6, the temperature and output were changed, and the joining conditions were confirmed. It was found that low temperature and low output resulted in failure of the joining process. In this manuscript we used the condition of 240 °C and 5W as a sufficient condition for joining. FW method was conducted as follows: A Li disc was put on the LLZ disc and heated with a small pressure at 240 °C for 5 min on a hotplate.

Characterization

SEM observation of the fracture cross-section was performed on a Jeol JCM-6000 Plus NeoScope instrument. XPS measurements were performed on a ULVAC-PHI VersaProbe II instrument with a monochromatic AlKα X-ray source (1486.6 eV). Before measurements, excess Li was removed by slicing a knife. The depth profile was obtained by using Ar^+ ion etching. The Li–LLZ interface was exposed by the Ar^+ ion etching and then measured.

Electrochemical impedance spectroscopy experiments were performed using laminate cells. An impedance analyser (Solartron 1470 coupled with Solartron 1260) was used, and a small perturbation voltage of 10 mV in the frequency range of 1 MHz to 1 Hz was applied for the measurements. High frequency impedance measurement was performed using a system (4990EDMS-120K, Toyo Corp.) A small perturbation voltage of 10 mV in the frequency range of 100 MHz to 20 Hz was applied. The Li plating and stripping measurements were conducted using a Solartron 1470 potentiostat/galvanostat. Constant positive and negative currents were both applied for 30 min per cycle.

Battery characterization

The Li (or Li–LLZ)|1 M LiTFSI in TEGDME|$LiFePO_4$ cells were assembled in HS cells (Hohsen Corp.). A commercial $LiFePO_4$ electrode (Hohsen Corp.) with a capacity of 1.5 mAh cm^{-2} was used. Whatman glass fiber membrane was used as a separator for 1 M LiTFSI in TEGDME. The Li|LLZ|catalytic electrode cell was assembled using a procedure similar to one previously reported[21]. The catalytic electrode containing LAGP particles and carbon nanotube was formed on the LLZ disc by sintering at 300 °C. Then, Li metal was formed on the other side of LLZ disc by the UFW method. The side of Li electrode was sealed by a plastic film like a laminate cell. The Li–O_2 cell was measured under a flow of oxygen gas in a vessel. The charge–discharge measurements were conducted using an device (HJ1001SD8, Hokuto Denko Co.).

Conflicts of interest

There are no conflicts to declare.

Acknowledgements

This work was partially conducted on the basis of the International joint research program for innovative energy technology by Ministry of Economy, Trade and Industry, Japan. A part of this work was supported by JSPS KAKENHI Grant Number JP15K18241. A part of this work was supported by JST ALCA-SPRING Project. A part of this work was supported by Murata Science Foundation. We are thankful to Inorganic Chemistry group of Osaka Prefecture University for providing the Li_3PS_4 powder. XPS measurements were carried out at National Institute for Materials Science (NIMS) Battery Research Platform.

Notes and references

1 Y. Kato, S. Hori, T. Saito, K. Suzuki, M. Hirayama, A. Mitsui, M. Yonemura, H. Iba and R. Kanno, *Nat. Energy,* 2016, **1**, 16030.
2 J. -M. Tarascon and M. Armand, *Nature,* 2001, **414**, 359.
3 M. Nakayama, T. Usui, Y. Uchimoto, M. Wakihara and M. Yamamoto, *J. Phys. Chem. B*, 2005, **109**, 4135.
4 P. Hartmann, T. Leichtweiss, M. R. Busche, M. Schneider, M. Reich, J. Sann, P. Adelhelm and J. Janek, *J. Phys. Chem. C,* 2013, **117**, 21064.
5 R. Murugan, V. Thangadurai and W. Weppner, *Angew. Chem. Int. Ed.,* 2007, **46**, 7778.
6 M. Nakayama, M. Kotobuki, H. Munakata, M. Nogami and K. Kanamura*, Phys. Chem. Chem. Phys.,* 2014, **14**, 10008.
7 L. E. Camacho-Forero and P. B. Balbuena, *J. Power Sources,* 2018, **396**, 782.
8 J. Wolfenstine, J. L. Allen, J. Read and J. Sakamoto, *J. Mater. Sci.,* 2013, **48**, 5846.
9 A. Sharafi, E. Kazyak, A. L. Davis, S. Yu, T. Thompson, D. J. Siegel, N. P. Dasgupta and J. Sakamoto*, Chem. Mater*., 2017, **29**, 7961.
10 L. Cheng, E. J. Crumlin, W. Chen, R. Qiao, H. Hou, S. F. Lux, V. Zorba, R. Russo, R. Kostecki, Z. Liu, K. Persson, W. Yang, J. Cabana, T. Richardson, G. Chen and M. Doeff, *Phys. Chem. Chem. Phys.,* 2014, **16**, 18294.
11 X. Han, Y. Gong, K. Fu, X. He, G. T. Hitz, J. Dai, A. Pearse, B. Liu, H. Wang, G. Rubloff, Y. Mo, V. Thangadurai, E. D. Wachsman and L. Hu*, Nat. Mater*., 2017, **16**, 573.
12 H. Huo, Y. Chen, R. Li, N. Zhao, J. Luo, J. G. P. da Silva, R. Mücke, P. Kaghazchi, X. Guo and X. Sun, *Energy Environ. Sci.,* 2020, **13**, 127.
13 J. E. Mcdonald and J. G. Eberhart*, Trans. Mettall. Soc. AIME,* 1965, **233**, 512.
14 D. Yonekura, T. Ueki, K. Tokiyasu, S. Kira and T. Wakabayashi*, Mater. Des.,* 2015, **65**, 907.
15 .A. Sakuda, A. Hayashi and M. Tatsumisago, *Chem. Mater*., 2010, **22**, 949.
16 B. Philippe, R. Dedryvére, J. Allouche, F. Lindgren, M. Gorgoi, H. Rensmo, D. Gonbeau and K. Edström, *Chem. Mater.,* 2012, **24**, 1107.
17 S. Wenzel, S. Randau, T. Leichtweiß, D. A. Weber, J. Sann, W. G. Zeier and J. Janek*, Chem. Mater.,* 2016, **28**, 2400.
18 S. J. Visco, E. Nimon, L. C. D. Jonghe, B. Katz and M.-Y. Chu, The 12th International Meeting on Lithium Batteries Abstracts, 2004, Abstract 396.

19 S. Wu, Y. Qiao, S. Yang, M. Ishida, P. He and H. Zhou*, Nat. Commun.,* 2017, **8**, 15607.
20 H. Xu, S. Wang and A. Manthiram, *Adv. Energy Mater.,* 2018, **8**, 1800813.
21 H. Kitaura and H. Zhou, *Energy Environ. Sci.,* 2012, **5**, 9077.
22 H. Kitaura and H. Zhou, *Sci. Rep.,* 2015, **5**, 13271.
23 X. B. Zhu, T. S. Zhao, Z. H. Wei, P. Tan and G. Zhao*, Energy Environ. Sci.,* 2015, **8**, 2782.
24 Y. Suzuki, K. Watanabe, S. Sakuma and N. Imanishi, *Solid State Ionics,* 2016, **289**, 72.
25 S. Chereddy, P. R. Chinnam, V. Chatare, S. P. di Luzio, M. P. Gobet, S. G. Greenbaum and S. L. Wunder*, Mater. Horiz.,* 2018, **5**, 461.
26 J. -L. Shui, J. S. Okasinski, P. Kenesei, H. A. Dobbs, D. Zhao, J. D. Almer and D. -J. Liu*, Nat. Commun.,* 2013, **4**, 2255.
27 P. G. Bruce, S. A. Freunberger, L. J. Hardwick and J. -M. Tarascon, *Nat. Mater.,* 2012, **11**, 19.
28 J. Lu, T. Wu and K. Amine, *Nat. Energy,* 2017, **2**, 17011.